Interfacial energy of solid In_2Bi intermetallic phase in equilibrium with In–Bi eutectic liquid at 72 °C equilibrating temperature

S. Akbulut[a], Y. Ocak[a,b], N. Maraşlı[b,*], K. Keşlioğlu[b], U. Böyük[a,c], E. Çadırlı[d], H. Kaya[c]

[a]Erciyes University, Institute of Science and Technology, Department of Physics, 38039 Kayseri—Turkey
[b]Erciyes University, Faculty of Arts and Sciences, Department of Physics, 38039 Kayseri—Turkey
[c]Erciyes University, Education Faculty, Department of Science Education, 38039 Kayseri—Turkey
[d]Niğde University, Faculty of Arts and Sciences, Department of Physics, Niğde—Turkey

ARTICLE DATA

Article history:
Received 20 August 2007
Accepted 30 August 2007

Keywords:
In_2Bi intermetallic phase
Crystal growth
Interfacial energy
Grain boundary energy
Thermal conductivity

ABSTRACT

A radial temperature gradient on the sample was established by heating from centre with a single heating wire and cooling the outside of sample at −10 °C with a heating/refrigerating circulating bath containing an aqueous ethylene glycol solution. The equilibrated grain boundary groove shapes of solid In_2Bi (In-33.2 at.% Bi) in equilibrium with In–Bi eutectic liquid (In-22 at.% Bi) were observed from quenched sample at 72 °C. Gibbs–Thomson coefficient and solid–liquid interfacial energy of solid In_2Bi in equilibrium with In–Bi eutectic liquid have been determined to be $(11.3\pm0.6)\times10^{-8}$ K m and $(47.8\pm4.8)\times10^{-3}$ J m^{-2} from the observed grain boundary groove shapes. The grain boundary energy of solid In_2Bi phase has been calculated to be $(92.8\pm10.2)\times10^{-3}$ J m^{-2} by considering a force balance at the grain boundary grooves. The thermal conductivities of solid In solution (In-12.4 at.% Bi), solid In_2Bi (In-33.2 at.% Bi), the eutectic liquid phase (In-22 at.% Bi) and their ratio at 72 °C have also been measured with radial heat flow apparatus and Bridgman type growth apparatus.

1. Introduction

The solid–liquid interfacial energy, σ_{SL}, is the reversible work required to form or to extend a unit area of interface between a crystal and its coexisting liquid and plays a central role in determining the nucleation rate and growth morphology of crystals [1–3]. Thus, a quantitative knowledge of σ_{SL} values is necessary. The measurement of σ_{SL} in pure materials and alloys is difficult. Over the last half-century, various attempts have been made to determine the mean value of solid–liquid interfacial free energy in variety of materials [1–22]. More recently, a technique for the quantification of interfacial free energy from the solid–liquid interfacial grain boundary groove shape has been established, and measurements have been reported for several systems [7–22]. These measurements of groove shape in a thermal gradient can be used to determine the interfacial energy, independent of the grain boundary energy because the interface near the groove must everywhere satisfy

$$\Delta T_r = \left[\frac{1}{\Delta S_f}\right]\left[\left(\sigma_{SL}+\frac{d^2\sigma_{SL}}{d_{n_1^2}}\right)\kappa_1+\left(\sigma_{SL}+\frac{d^2\sigma_{SL}}{d_{n_2^2}}\right)\kappa_2\right] \quad (1)$$

where ΔT_r, is the curvature undercooling, ΔS_f is the entropy of fusion per unit volume, $n=(n_x, n_y, n_z)$ is the interface normal, κ_1 and κ_2 are the principal curvatures, and the derivatives are taken along the directions of principal curvature. Thus, the curvature undercooling is a function of curvature, interfacial free energy and the second derivative of the interfacial free

* *Corresponding author*. Tel.: +90 352 4374901x33114; fax: +90 352 437 49 33.
E-mail address: marasli@erciyes.edu.tr (N. Maraşlı).

1044-5803/$ – see front matter © 2007 Elsevier Inc. All rights reserved.
doi:10.1016/j.matchar.2007.08.028

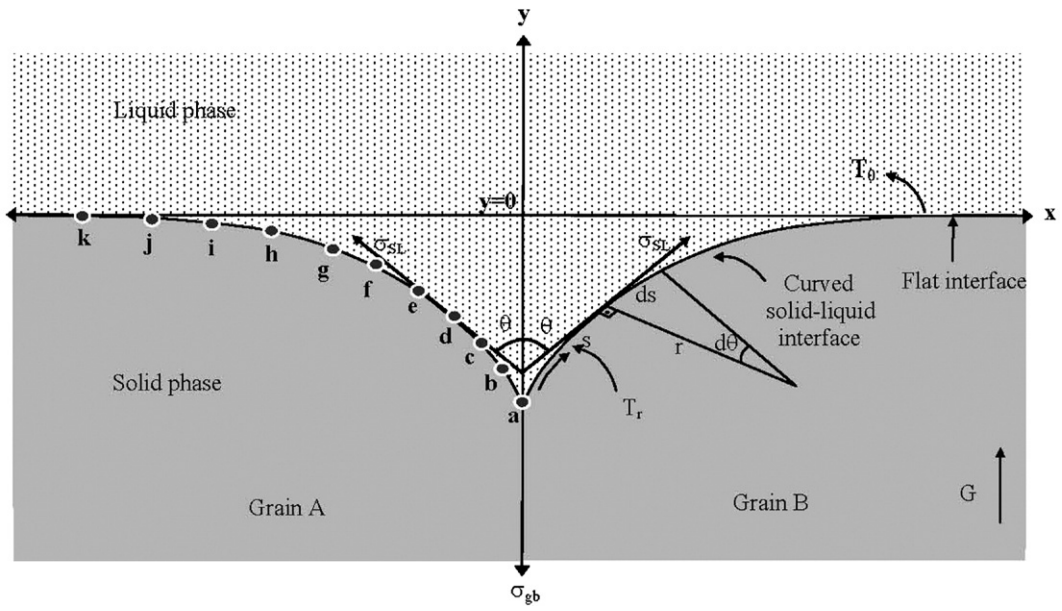

Fig. 1 – Schematic illustration of an equilibrated grain boundary groove formed at a solid–liquid interface in a temperature gradient showing the definitions of r, θ and y in Eq. (5).

energy. Eq. (1) is valid only if the interfacial free energy per unit area is equal to surface tension per unit length, $\sigma_{SL}=\gamma$. When surface energy differs from surface tension, the problem is more complicated and the precise modification of the Gibbs–Thomson equation is not yet established [4]. When the solid–liquid interfacial free energy is isotropic, Eq. (1) becomes

$$\Delta T_r = \frac{\sigma_{SL}}{\Delta S_f}\left(\frac{1}{r_1}+\frac{1}{r_2}\right) \tag{2}$$

where r_1 and r_2 are the principal radii of curvature. For the case of a planar grain boundary intersecting a planar solid–liquid interface, $r_2=\infty$ and the Eq. (2) becomes

$$\Gamma = r\Delta T_r = \frac{\sigma_{SL}}{\Delta S_f} \tag{3}$$

where Γ is the Gibbs–Thomson coefficient. This equation is called the Gibbs–Thomson relation. Eq. (3) may be integrated in the y direction (perpendicular to the macroscopic interface) from the flat interface to a point on the cusp

$$\int_0^{-y} \Delta T_r dy = \Gamma \int_0^{-y} \frac{1}{r} dy. \tag{4}$$

The right hand side of Eq. (4) may be evaluated for any shape by noting that by definition of $ds=r\,d\theta$ and $dy=r\cos\theta\,d\theta$ (s and θ are shown in Fig. 1) so that

$$\Gamma \int_0^{-y} \frac{1}{r} dy = -\Gamma \int_0^{y} \frac{1}{r} dy = -\Gamma \int_{\pi/2}^{\theta} \frac{1}{r} r\cos\theta d\theta = \Gamma(1-\sin\theta). \tag{5}$$

The left-hand side of Eq. (4) may be evaluated if ΔT_r is known as a function of y. When the thermal conductivities of solid and liquid phases are equal, the temperature just depends on temperature gradient and the distance: that is

$$\Delta T_r = Gy \tag{6}$$

so that

$$\frac{1}{2}Gy^2 = \Gamma(1-\sin\theta). \tag{7}$$

The value of Γ may be obtained from the slope of a plot of y^2 against $(1-\sin\theta)$. Theoretical basis of grain boundary groove profile method was given by Bolling and Tiller [5] for equal thermal conductivities of solid and liquid phases and the first report of its application to measure σ_{SL} was by Jones and Chadwick [6] for some transparent materials. Nash and Glicksman [7] have extended Bolling and Tiller's analysis to include the effects of unequal thermal conductivities of solid and liquid phases. Measurements of solid–liquid interfacial energies were made for some transparent organic materials [5–11].

The technique was extended to measure σ_{SL} for alloys by Gündüz and Hunt [12,13]. Observation of grain boundary groove shape in an alloy is obviously very difficult. Gündüz and Hunt [12] have developed an apparatus to obtain grain boundary groove shape in binary eutectic systems. The details of apparatus and experimental procedures are given in Ref. [12]. Gündüz and Hunt [12] also developed a finite difference model to calculate the correspondence difference in temperature, ΔT_r between the flat interface for each points on the grain boundary groove shapes and evaluated the right hand side of the Eq. (4) by measuring the values of theta, θ. The values of theta,θ was obtained by fitting a Taylor expansion to the adjacent points on the cusp. Usually the points from b to i shown in (Fig. 1) were used to obtain more reliable Γ values with Gündüz and Hunt's model. This numerical method calculates the temperature along the interface of a measured grain boundary groove shape rather than attempting to predict the equilibrium grain boundary groove shape. If the grain boundary groove shape, the temperature gradient in the solid, G_S and the ratio of thermal conductivity of the equilibrated liquid phase to solid phase, $R=K_L/K_S$ is known or measured the value of the Gibbs–Thomson coefficient is then obtained with the Gündüz and Hunt numerical method. Measurements of the solid–liquid interface energies were made in metallic binary eutectic based systems [12–18].

Bayender et al [19] designed an apparatus to directly observe equilibrated grain boundary groove shape for transparent

materials. They applied Gündüz and Hunt's numerical method to determine Gibbs–Thomson coefficients, solid–liquid interface energies and grain boundary energies. Measurements of the solid–liquid interface energies were made in transparent organic binary systems [19–22].

The measurements of solid–liquid interfacial energies in metallic binary alloys having low melting temperature were not made because of the difficulty of temperature control on the sample and worries about quenching of interface at the low equilibrating temperature. Thus the aims of the present work were to observe the grain boundary groove shapes in metallic alloys at the low equilibrating temperature and to determine the Gibbs–Thomson coefficient, solid–liquid interfacial energy and grain boundary energy for solid In_2Bi (In-33.2 at.% Bi) in equilibrium with the eutectic liquid (In-22 at.% Bi) from the observed grain boundary groove shapes.

2. Experimental procedure

2.1. *Experimental apparatus*

To observe the equilibrated grain boundary groove shapes in opaque materials, Gündüz and Hunt [12] designed a radial heat flow apparatus. Maraşlı and Hunt [14] improved the experimental apparatus for higher temperature. The details of the apparatus and experimental procedures are given in Refs. [12–14]. In the experimental technique, the sample was heated from centre by single heating wire and the outside of the sample was kept cool by water cooling to get a constant radial temperature gradient on the sample. A thin liquid layer was melted around the central heating wire and annealed for an enough period in a constant radial temperature gradient. At the end of annealing period, the sample was quenched by just cutting off power. The cooling of the sample from outside must be more effective to get well quenched solid–liquid interface. The water cooling was sufficient to get well defined solid–liquid interface at the high equilibrating temperature but after a few experimental works it was seen that the water cooling was not sufficient to get well defined solid–liquid interface at the lower equilibrating temperature which is smaller then 140 °C. Melting point of In-22 at.% Bi eutectic alloy is 72 °C. Thus, the outside of sample was kept at −10 °C using a *Poly Science digital 9102* model heating/refrigerating circulating bath containing an aqueous ethylene glycol solution and the gap between the cooling jacket and sample was filled with graphite dust to get well quenched solid–liquid interface in the present work. The temperature of circulating baths was kept constant at −10 °C to an accuracy of ±0.01 K and the temperature on the sample was controlled to an accuracy of ±0.01 K with a *Eurotherm 2604* type controller.

2.2. *Sample production*

Consider a binary eutectic system. Above the eutectic temperature, a binary eutectic system consists of solid and liquid provided the alloy composition, $C_\alpha < C_0 < C_E$ or $C_E > C_0 < C_\beta$. Where C_E, C_α, and C_β are the composition of the eutectic, solid α and solid β phases, respectively. If this eutectic system is held in a very stable temperature gradient, the liquid droplets move up the temperature gradient by temperature gradient zone melting (TGZM) and single solid can grow on the eutectic structure during the annealing period. When the composition of alloy is far from the eutectic composition, the experiment usually needs a long time to reach equilibrium due to larger freezing range. If the alloy composition is near the eutectic composition, above the eutectic temperature, a binary eutectic system consists of liquid. If this system is held in a very stable temperature gradient there will be no liquid droplets behind the solid phase and two solid phases can grow together on the eutectic structure. Equilibrating time for this system should be shorter because of the small freezing range.

The composition of alloy was chosen to be In-33.2 at.% Bi to grow the single solid In_2Bi intermetallic phase from the eutectic liquid on the eutectic structures. In-33.2 at.% Bi alloy was prepared in a vacuum furnace by using 99.99% pure indium and 99.9% pure bismuth. After stirring, the molten alloy was poured into a graphite crucible held in a specially constructed casting furnace at approximately 30 K above the melting point of alloy. The molten metal was then directionally frozen from bottom to top to ensure that the crucible was completely full. The sample was then placed in the radial heat flow apparatus.

The experiments were carried out in two steps. In the first step, the thermocouples were calibrated by detecting the melting point during very slow heating and cooling using lower temperature gradient operational mode. In the second step, the specimen was heated from the centre using a single heating wire (1.7 mm in diameter, Kanthal A-1) and the outside of the specimen was kept at −10 °C using a *Poly Science digital 9102* model heating/refrigerating circulating bath containing an aqueous ethylene glycol solution. A thin liquid layer (1–2 mm thick) was melted around the central heater and the specimen was annealed in a very stable temperature gradient for a long time. The annealing time for In-33.2 at.% Bi alloy was 4 days. During the annealing period, the temperature in the specimen and the vertical temperature variations on the sample were continuously recorded by the stationary thermocouples and a moveable thermocouple, respectively with a data logger via computer and input power were recorded periodically. The temperature in the sample was stable to about ±0.025 K for hours and ±0.05 K for up to 4 days. At the end of the annealing time the specimen was rapidly quenched by turning off the input power which is sufficient to get a well defined solid–liquid interface, because the liquid layer around the central heating wire was very thin (typically less than 0.5–1 mm).

2.3. *Measurements of the coordinates of equilibrated grain boundary groove shapes*

The quenched sample was cut transversely into lengths typically 25 mm and transverse sections were ground flat with 180 grit SiC paper. Grinding and polishing were then carried out by following standard route. After polishing, the samples were etched with a 4 g Picric Acid $[(NO_2)_3C_6H_2OH]$ and 20 ml Hydrochloric acid [HCl] in 400 ml Ethanol $[C_2H_5OH]$ for 3 s.

The equilibrated grain boundary groove shapes were then photographed with a *Honeywell CCD* digital camera placed in conjunction with an *Olympus BH2* type light optical

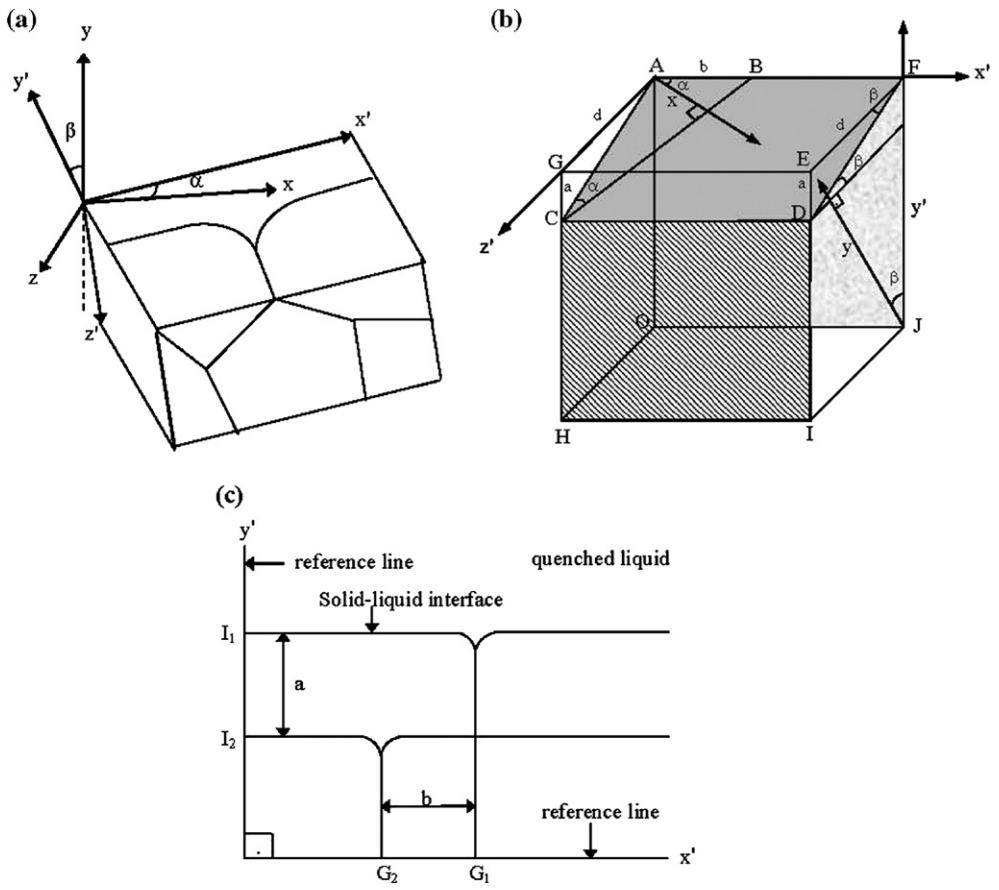

Fig. 2 – (a) Schematic illustration of the relationship between the actual coordinates, x, y and the measured coordinates, x′, y′ of the groove shape; (b) Schematic illustration for the metallic examination of the sample: where B is the location of the grain boundary groove shape onto first plane OJFA, C is the location of the grain boundary groove shape onto second plane HIDC, AB=b, CO=ED=a and AG=d; (c) Schematic illustration of the displacement of the grain boundary groove shape position along the x′ and y′ axis [14].

microscope. A graticule (200×0.01=2 mm) was also photographed using the same objective. The photographs of the equilibrated grain boundary groove shapes and the graticule were superimposed on one another using *Adobe PhotoShop 8.0* version software so that accurate measurement of the groove coordinate points on the groove shapes could be made.

2.4. *Geometrical correction for the groove coordinates*

The coordinates of the cusp, x, y should be measured using the coordinates x, y, z where the x axis is parallel to the solid–liquid interface, the y axis is normal to the solid–liquid interface and the z axis lies at the base of the grain boundary groove as shown in (Fig. 2(a)). The coordinates of the cusp x′, y′ from the metallographic section must be transformed to the x, y coordinates. Maraşlı and Hunt [14] devised a geometrical method to make appropriate corrections to the groove shapes and the details of the geometrical method are given in Ref. [14].

The relation between x and x′ can be expressed as [14]

$$x = x'\cos\alpha$$

$$x = x'\frac{\sqrt{a^2+d^2}}{\sqrt{a^2+b^2+d^2}} \tag{8}$$

and the relation between y and y′ can be expressed as [14]

$$y = y'\cos\beta$$

$$y = y'\frac{d}{\sqrt{a^2+d^2}} \tag{9}$$

where d is the distance between the first and second plane along the z′ axis, b is the displacement of the grain boundary position along the x′ axis, a is the displacement of the solid–liquid interface along the y′ axis, α is the angle between the x′ axis and x axis, and β is the angle between the y′ axis and y axis as shown in (Fig. 2). In this work, the values of a, b and d were measured in order to transform the cusps coordinates x′, y′ into the x, y coordinates as follows.

Two perpendicular reference lines (approx. 0.1 mm thick and 0.1 mm deep) were marked near the grain boundary groove on the polished surface of sample (Fig. 2c). The samples were then polished and the grain boundary groove shapes were photographed. The thickness of the sample d_1 was measured with a digital micrometer (resolution of 1 μm) at several points of the sample to obtain the average value. After thickness measurements had been made the sample was again polished to remove a thin layer (at least 40–50 μm) from the sample surface. The same grain boundary groove

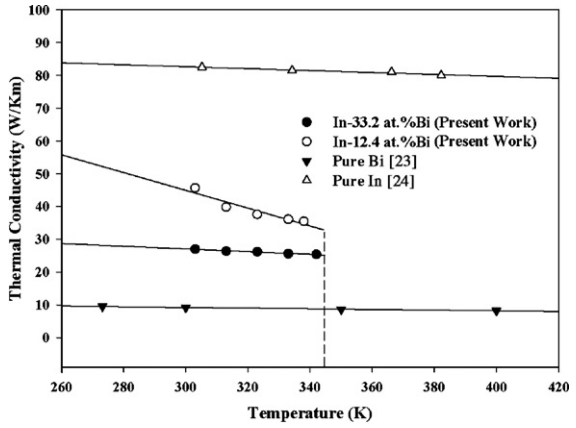

Fig. 3 – Thermal conductivities of solid Indium solution and solid In_2Bi intermetallic phases versus time at the eutectic temperature. ●, In-33.2 at.%Bi (Present Work); ○, In-12.4 at.%Bi (Present Work); ▼, Pure Bi [23]; △, Pure In [24].

shapes were again photographed and the thickness of the sample d_2 was measured with the same micrometer. The difference between the thickness of the sample, $d=d_1-d_2$ gave the layer removed from the sample surface. The photographs of the grain boundary groove shapes were superimposed on one another using *Adobe PhotoShop 8.0* version software to measure the displacement of the solid–liquid interface along the y' axis and the displacement of the grain boundary groove position along the x' axis (see Fig. 2b). Thus the required a, b and d measurements were made so that appropriate corrections to the shape of the grooves could be deduced [14].

The coordinates of equilibrated grain boundary groove shapes were measured with an optical microscope to an accuracy of ±10 μm. The thickness of the sample (2–2.5 cm lengths) for geometrical correction was measured with a digital micrometer which has ±1 μm resolution. Thus the uncertainty in the measurements of equilibrated grain boundary coordinates was less than 0.2%.

2.5. *Thermal conductivities of the solid and liquid phases*

The thermal conductivity ratio of the eutectic liquid phase (In-22 at.% Bi) to solid In_2Bi (In-22 at.% Bi) intermetallic phase, $R=K_{L(\text{eutectic liquid})}/K_{S(\text{intermetallic})}$ must be known or measured to evaluate the Gibbs–Thomson coefficients with the present numerical method. The radial heat flow apparatus is an ideal technique for measuring the thermal conductivity of the solid phases. The thermal conductivities of solid In solution (In-12.4 at.% Bi), solid In_2Bi (In-22 at.% Bi) and eutectic liquid (In-12.4 at.% Bi) are also needed to evaluate the thermal conductivity ratio of equilibrated eutectic liquid phase to solid In_2Bi phase and the temperature gradient on the solid phase. In the radial heat flow method, a cylindrical sample was heated by using a single heating wire along the axis at the centre of the sample and the sample was kept in a very stable temperature gradient for a period to achieve the steady state condition. At the steady-state condition, the temperature gradients in the cylindrical specimen is given by Fourier's law

$$\frac{dT}{dr}=-\frac{Q}{AK_S} \tag{10}$$

where Q is the total input power from the centre of the specimen, A is the surface area of the specimen and K_S is the thermal conductivity of the solid phase. Integration of Eq. (10) gives

$$K_S=\frac{1}{2\pi\ell}\ln\left(\frac{r_2}{r_1}\right)\frac{Q}{T_1-T_2} \tag{11}$$

$$K_S=a_0\frac{Q}{T_1-T_2} \tag{12}$$

where $a_0=\ln(r_2/r_1)/2\pi\ell$ is an experimental constant, r_1 and r_2 ($r_2>r_1$) are fixed distances from the centre axis of the specimen, ℓ is the length of the heating wire which is constant and T_1 and T_2 are the temperatures at the fixed positions, r_1 and r_2 from the centre axis of the specimen. Eq. (12) could be used to obtain the conductivity of the solid phase by measuring the difference in temperature between the two fixed points for a given power level provided that the vertical temperature variation is minimum or zero.

The thermal conductivities of the solid In-12.4 at.% Bi and solid In-33.2 at.% Bi phases were measured in the radial heat flow apparatus. The alloy was prepared in a vacuum furnace by using 99.99% purity Indium and 99.9% purity Bismuth. The sample was heated using the central heating wire in steps of from 303.2 K up to 5 K below the eutectic temperature (345.15 K). The samples were kept at steady-state for at least 2 h. At steady-state condition, the total input power, vertical temperature variations on the sample and the temperatures in the sample were measured. When all desired power and temperature measurements had been completed the sample was left to cool down to room temperature.

The thermal conductivities of solid In solution (In-12.4 at.% Bi) and solid In_2Bi (In-33.2 at.% Bi) phases versus temperature are shown in (Fig. 3). The values of K_S for the solid In solution and solid In_2Bi phases at the eutectic melting temperature

Table 1 – Thermal conductivities of solid and liquid phases and their ratios at their melting temperatures for In–Bi binary eutectic system

Alloy	Phases	Melting temperature (K)	K (W/K m)	$R=K_L/K_S$
In–Bi eutectic	Eutectic liquid (In-22 at.% Bi)	345.15	27.56	0.84
	Solid In solution (In-12.4 at.% Bi)	345.15	32.82	
	Eutectic liquid (In-22 at.% Bi)	345.15	27.56	1.09
	Solid (In-33.2 at.% Bi)	345.15	25.21	

were obtained to be 32.82 and 25.21 W/Km, respectively by extrapolating to the eutectic temperature as shown in (Fig. 3). The values of thermal conductivities used in the calculations are given in Table 1.

The thermal conductivity of eutectic liquid phase at the eutectic temperature is needed to evaluate the thermal conductivity ratio of equilibrated eutectic liquid phase to solid In_2Bi intermetallic phase. It is not possible to measure the thermal conductivity of the liquid phase with the radial heat flow apparatus since a thick liquid layer (10 mm) is required. A layer of this size would certainly have led to convection. If the thermal conductivity ratio of the eutectic liquid phase (In-22 at.% Bi) to the solid In solution phase (In-12.4 at.% Bi) is known and the thermal conductivity of the solid In solution phase (In-12.4 at.% Bi) phase is measured at the melting temperature, the thermal conductivity of the eutectic liquid phase can then be evaluated. The thermal conductivity ratio can be obtained during directional growth with a Bridgman type growth apparatus. The heat flow away from the interface through the solid phase must balance that liquid phase plus the latent heat generated at the interface, i.e. [25]

$$VL = K_S G_S - K_L G_L \tag{13}$$

where V is the growth rate, L is the latent heat, G_S and G_L are the temperature gradients in the solid and liquid, respectively and K_S and K_L are the thermal conductivities of solid and liquid phases, respectively. For very low velocities, $VL \ll K_S G_S$, so that the thermal conductivity ratio, R is given by

$$R = \frac{K_L}{K_S} = \frac{G_S}{G_L} \tag{14}$$

A directional growth apparatus, firstly constructed by McCartney [26], was used to find out the thermal conductivity ratio, $R = K_L/K_S$. A thin walled graphite crucible, 6.3 mm OD × 4 mm ID × 180 mm length, was used to minimize convection in the liquid phase.

Molten In-12.4 at.% Bi alloy was poured into the thin walled graphite tube and the molten alloy was then directionally frozen from bottom to top to ensure that the crucible was completely full. The specimen was then placed in the directional growth apparatus. The specimen was heated to 30 K over the melting temperature of alloy. The specimen was then left to reach thermal equilibrium for at least 2 h. The temperature in the specimen was measured with an insulated K type thermocouple. In the present work, 1.2 mm OD × 0.8 mm ID alumina tube was used to insulate the thermocouple from the melt and the thermocouple was placed perpendicular to the heat flow (growth) direction. At the end of equilibration, the temperature in the specimen was stable to ±0.5 K for short term period and to ±1 K for long term period. When the specimen temperature stabilized, the directional growth was begun by turning the motor on. The cooling rate was recorded with a data logger via computer. In the present measurements, the growth rate was 8.3×10^{-4} cm/s. When the solid–liquid interface passed the thermocouple, a change in the slope of the cooling rate for liquid and solid phases was observed. When the thermocouple reading was approximately 30 K below the melting temperature, the growth was stopped by turning the motor off.

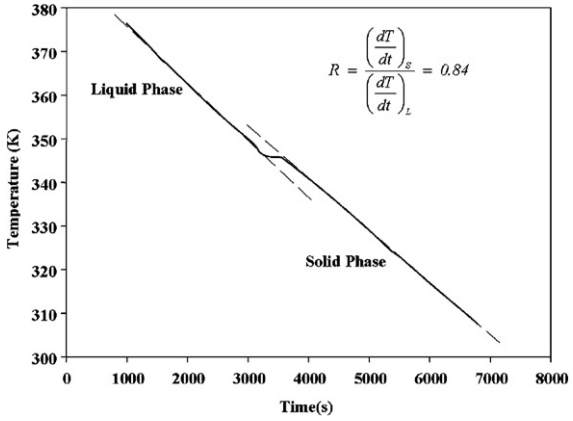

Fig. 4 – Cooling rate of In-12.4 at.% Bi alloy.

The conductivity ratio can be evaluated from the cooling rate ratio of liquid phase to solid phase. The cooling rate of the liquid and solid phases is given by

$$\left(\frac{dT}{dt}\right)_L = \left(\frac{dT}{dx}\right)_L \left(\frac{dx}{dt}\right)_L = G_L V \tag{15}$$

and

$$\left(\frac{dT}{dt}\right)_S = \left(\frac{dT}{dx}\right)_S \left(\frac{dx}{dt}\right)_S = G_S V. \tag{16}$$

From Eqs. (14), (15) and (16), the conductivity ratio can be written as

$$R = \frac{K_L}{K_S} = \frac{G_S}{G_L} = \frac{\left(\frac{dT}{dt}\right)_S}{\left(\frac{dT}{dt}\right)_L} \tag{17}$$

where $(dT/dt)_S$ and $(dT/dt)_L$ values were directly measured from the temperature versus time curve shown in (Fig. 4). The thermal conductivity ratio of the eutectic liquid (In-22 at.% Bi) to the solid In solution (In-12.4 at.% Bi), $R = K_{L(\text{eutectic liquid})}/K_{S(\text{solid In solution})}$ was found to be 0.84 as shown in (Fig. 4). The thermal conductivity of the solid In solution and solid In_2Bi phases at the eutectic melting temperature are also found to be 32.82 and 25.21 W/K m, respectively from (Fig. 3). The thermal conductivity of eutectic liquid phase (In-22 at.% Bi) is found to be 27.56 W/K m from value of R for In-12 at.% Bi alloy. Thus the thermal conductivity ratio of equilibrated eutectic liquid phase (In-22 at.% Bi) to solid In_2Bi intermetallic phase, $R = K_{L(\text{eutectic liquid})}/K_{S(\text{solid intermetallic})}$ is evaluated to be 1.09. The values of K_L and K_S used in determination of Gibbs–Thomson coefficients are also given in Table 1.

The estimated experimental error in the measurement of K_S is sum of the fractional uncertainty of the measurements of power, temperature differences, length of heating wire and thermocouples positions which can be expressed as

$$\left|\frac{\Delta K_S}{K_S}\right| = \left|\frac{\Delta Q}{Q}\right| + \left|\frac{\Delta T_1}{T_1}\right| + \left|\frac{\Delta T_2}{T_2}\right| + \left|\frac{\Delta \ell}{\ell}\right| + \left|\frac{\Delta r_1}{r_1}\right| + \left|\frac{\Delta r_2}{r_2}\right| \tag{18}$$

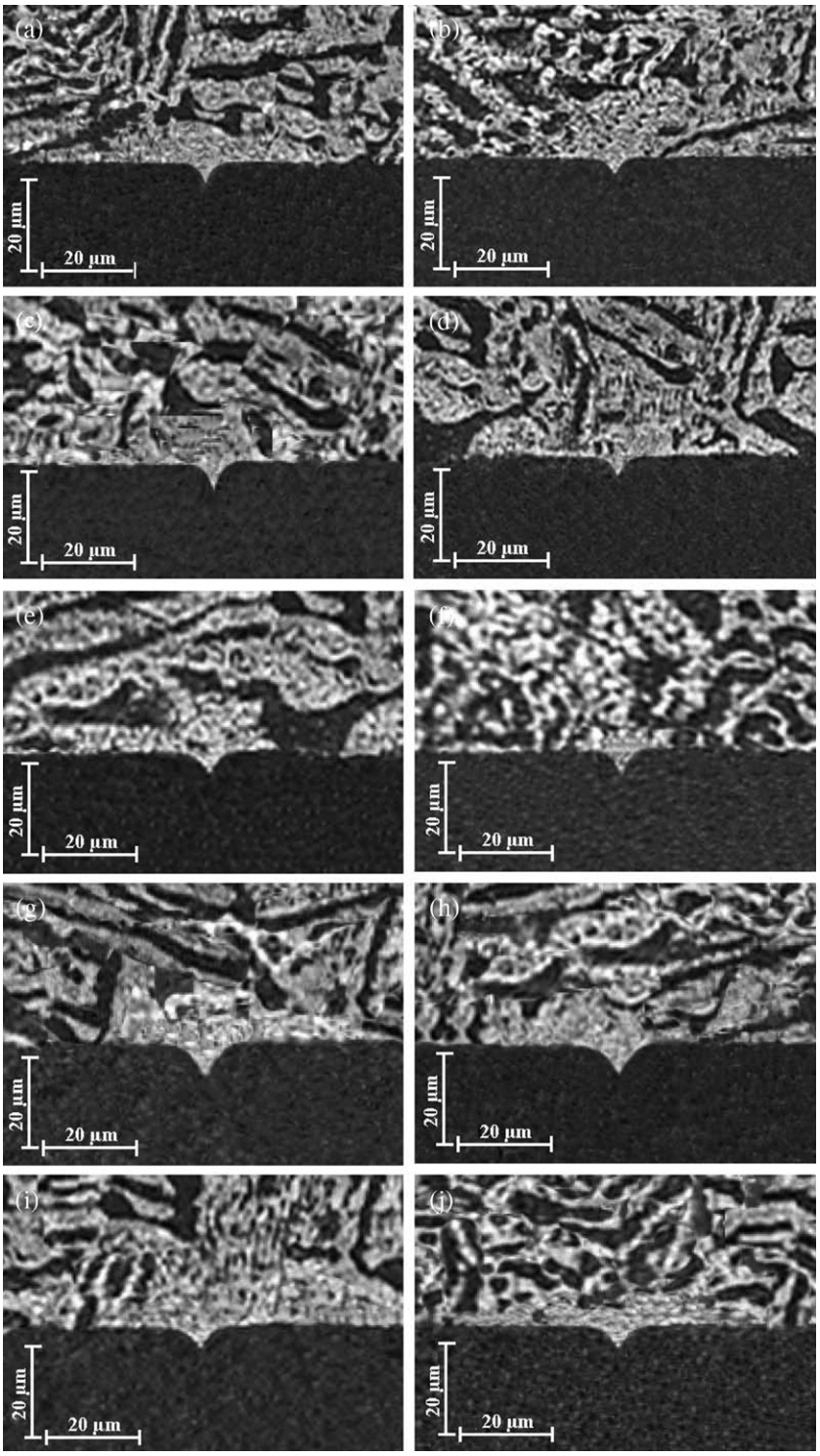

Fig. 5 – Typical grain boundary groove shapes for solid In_2Bi in equilibrium with In-33.2 at.% Bi eutectic liquid.

The estimated error in the thermal conductivity measurements is about 5% [27].

2.6. *Temperature gradient measurement in the solid phase*

The cylindrical sample was heated from the centre by a thin heating wire and a thin liquid layer was melted around the central heating element. At the steady-state the temperature gradient at radius r is given by

$$G_S = \frac{dT}{dr} = -\frac{Q}{2\pi r \ell K_S} \tag{19}$$

where Q is the input power, ℓ is the length of the heating element, r is the distance of the solid–liquid interface to the

Table 2 – The values of Gibbs–Thomson coefficient for solid In_2Bi (In-33.2 at.% Bi) in equilibrium with eutectic liquid (In-22 at.% Bi) determined in present work

Groove no	$G_S \times 10^2$ (K/m)	α^0	β^0	Gibbs–Thomson coefficient	
				$\Gamma_{LHS} \times 10^{-8}$ (Km)	$\Gamma_{RHS} \times 10^{-8}$ (Km)
a	31.4	10.3	8.9	11.5	11.0
b	31.9	11.5	8.5	11.1	10.5
c	32.8	14.3	9.9	11.2	11.7
d	33.1	8.9	8.1	11.4	10.2
e	28.8	6.3	8.5	12.1	11.1
f	26.9	5.7	10.6	11.8	11.0
g	29.6	7.3	10.6	11.4	11.8
h	28.6	12.3	10.9	10.9	11.3
i	28.2	8.9	12.3	10.5	12.3
j	31.3	10.9	9.2	12.1	11.9
				$\bar{\Gamma} = (11.3 \pm 0.6) \times 10^{-8}$ Km	

centre of the sample and K_S is the thermal conductivity of the solid phase.

The average temperature gradient of the solid phase must be determined for each grain boundary groove shape. This was done by measuring the input power, the length of heating element, the position of the solid–liquid interface and the value of K_S for the solid In_2Bi phase at the eutectic melting point. By using these measured values in Eq. (19), temperature gradient can be determined for each grain boundary groove shape.

The estimated experimental error in the measurement of temperature gradient is the sum of the fractional uncertainty of the measurements of power, length of heating wire, thermal conductivity and thermocouples positions which can be expressed as

$$\left|\frac{\Delta G_S}{G_S}\right| = \left|\frac{\Delta Q}{Q}\right| + \left|\frac{\Delta \ell}{\ell}\right| + \left|\frac{\Delta r}{r}\right| + \left|\frac{\Delta K_S}{K_S}\right|. \tag{20}$$

If Eq. (20) is compared with Eq. (18), the experimental errors came from the measurements of Q, ℓ, r ΔT in Eq. (20) already exist in the fractional uncertainties at Eq. (18). Thus the total experimental error in the thermal gradient measurements is equal to the experimental error in thermal conductivity measurements and is about 5%.

3. Results and discussions

3.1. Determination of Gibbs–Thomson coefficient

If the thermal conductivity ratio of the liquid phase to the solid phase, the coordinates of the grain boundary groove shapes and the temperature gradient of the solid phase are known, the Gibbs–Thomson coefficient (Γ) can be obtained using the numerical method described in detail in Ref. [12]. The experimental error in the determination of Gibbs–Thomson coefficient is the sum of experimental errors in the measurements of the temperature gradient, thermal conductivity and groove coordinates. Thus the total error in the determination of Gibbs–Thomson coefficient is about 5%.

In the present work, the Gibbs–Thomson coefficients for the solid In_2Bi in equilibrium with In-22 at.% Bi eutectic liquid were determined with the present numerical model by using ten equilibrated grain boundary groove shapes. The grooves examined in this system are shown in (Fig. 5). As can be seen from (Fig. 5), a solid In solution phase (In-12.4% at. Bi) first nucleates on the surface of the solid In_2Bi intermetallic phase, then both solid In solution and In_2Bi intermetallic phases grow together to form a eutectic grain. This allows a well defined and fixed solid–liquid interface to be observed during the quench and also the phases, grains and interfaces of the system are very clear. The values of Γ for solid In_2Bi are given in Table 2. The average value of Γ from Table 2 is $(11.3 \pm 0.6) \times 10^{-8}$ K m for solid In_2Bi in equilibrium with In-22 at.% Bi eutectic liquid.

3.2. Determination of entropy of fusion per unit volume

It is also necessary to know the entropy of fusion per unit volume, ΔS_f for solid phase determine the solid–liquid interfacial energy. For pure materials the entropy of fusion per unit volume is given by

$$\Delta S_f = \frac{\Delta H_M}{T_M} \frac{1}{V_S} \tag{21}$$

where ΔH_M is the enthalpy change of solid phase at melting temperature, T_M is the melting temperature and V_S is the molar volume of solid phase. The entropy change for an alloy is given by [12],

$$\Delta S_f = \frac{(1 - C_S)(S_A^L - S_A^S) + C_S(S_B^L - S_B^S)}{V_S} \tag{22}$$

where S_A^L S_A^S S_B^L and S_B^S are partial molar entropies for A and B materials and C_S is the solid composition. Since the entropy terms are generally not available, for convenience, the undercooling at constant composition may be related to the

Table 3 – Some physical properties of solid In_2Bi intermetallic (In-33.2 at.% Bi) phase at the eutectic temperature

System	In–Bi eutectic
Composition of the quenched liquid phase, C_L	In-22 at.% Bi [29]
Composition of solid In_2Bi phase, C_S	In-33.2 at.% Bi [29]
$f(C)$ [a]	0.65 [29]
Eutectic melting temperature, T_m (K)	345.15 [29]
Molar Volume of solid In_2Bi, V_{In2Bi} (m^3)	17.3×10^{-6} [29]
Liquidus slope, m_L (K/at.fr)	255.01 [29]
Entropy change of fusion for solid In_2Bi, ΔS_f (J/K m^3)	4.23×10^5

[a] $f(C) = \frac{C_S - C_L}{(1 - C_L)C_L}$

change in composition at constant temperature. For a sphere [28]

$$\Delta C_r = \frac{2\sigma_{SL} V_S (1 - C_L) C_L}{rRT_M (C_S - C_L)} \quad (23)$$

where R is the gas constant. For small changes

$$\Delta T_r = m_L \Delta C_r = \frac{2m_L \sigma_{SL} V_S (1 - C_L) C_L}{rRT_M (C_S - C_L)} \quad (24)$$

For spherical solid $r_1 = r_2 = r$ and the curvature undercooling is written by

$$\Delta T_r = \frac{2\sigma_{SL}}{r\Delta S_f} \quad (25)$$

From Eqs. (24) and (25), the entropy change for an alloy is written as

$$\Delta S_f = \frac{RT_M}{m_L V_S} \frac{C_S - C_L}{(1 - C_L) C_L}. \quad (26)$$

The values of the relevant constant obtained from Ref. [27] and the calculated entropy change of fusion per unit volume are given in Table 3. The error in the determined entropy change of fusion per unit volume is estimated to be about 5% [30].

3.3. *Evaluation of solid–liquid interfacial energy*

If the values of Γ and ΔS_f are known the value of solid–liquid interfacial energy, σ_{SL} can be evaluated from Eq. (3). The solid–liquid interfacial energy of the solid In_2Bi, in equilibrium with the eutectic liquid (In-22 at.% Bi) was evaluated to be $(47.8 \pm 4.8) \times 10^{-3}$ J m^{-2} using the values of Γ and ΔS_f. The experimental error in the determined solid–liquid interface energy is the sum of experimental errors of the Gibbs–Thomson coefficient and the entropy change of fusion per unit volume. Thus, the total experimental error of the solid–liquid interfacial energy evaluation in present work is about 10%.

3.4. *Grain boundary energy*

If the grains on either side of the interface are the same phase then the grain boundary energy can be expressed by

$$\sigma_{gb} = 2\sigma_{SL} \cos\theta \quad (27)$$

where $\theta = \frac{\theta_A + \theta_B}{2}$ is the angle that the solid–liquid interfaces make with the y axis. The angles, θ_A and θ_B were obtained from the cusp coordinates, x, y using a Taylor expansion for parts at the base of the groove. According to Eq. (27), the value of σ_{gb} should be smaller or equal to twice of solid–liquid interface energy, i.e. $\sigma_{gb} \leq 2\sigma_{SL}$.

The value of the grain boundary energy for the solid In_2Bi, σ_{gb} was found to be $(92.8 \pm 10.2) \times 10^{-3}$ J m^{-2} using the values of the σ_{SL} and θ into Eq. (27). The estimated error in determination of θ angles was found to be 1%. Thus the total experimental error in the resulting grain boundary energy is about 11%.

4. Conclusion

A radial temperature gradient on the sample was established by heating from centre with a single heating wire and cooling the outside of sample at −10 °C with a heating/refrigerating circulating bath containing an aqueous ethylene glycol solution. The equilibrated grain boundary groove shapes of solid In_2Bi (In-33.2 at.% Bi) in equilibrium with In–Bi eutectic liquid (In-22 at.% Bi) were observed from quenched sample at 72 °C. Gibbs–Thomson coefficient, solid–liquid interfacial energy and grain boundary energy for solid In_2Bi in equilibrium with In–Bi eutectic liquid have been determined from the observed grain boundary groove shapes. The thermal conductivities of solid In solution (In-12.4 at.% Bi), the solid In_2Bi phase, the eutectic liquid phase (In-22 at.% Bi) and their ratio at 72 °C have also been measured with radial heat flow apparatus and Bridgman type growth apparatus.

Acknowledgements

This research was financially supported by the Scientific and Technical Research Council of Turkey (TÜBİTAK under Contract No: 105T481). The Authors are grateful to Erciyes Scientific and Technical Research Council of Turkey (TÜBİTAK) for their financial support.

REFERENCES

[1] Turnbull DJ. Formation of crystal nuclei in liquid metals. Appl Phys 1950;21:1022.
[2] Jones DRH. The free energies of solid–liquid interfaces. J Mater Sci 1974;9:1.
[3] Jackson CL, McKenna GB. The melting behavior of organic materials confined in porous solids. J Chem Phys 1990;93:9002.
[4] Trivedi R, Hunt JD. The mechanics of solder alloy wetting and spreading. New York: Van Nostrand Reinhold; 1993. p. 191.
[5] Bolling GF, Tiller WA. Growth from the melt. I influence of surface intersection In pure metals. J Appl Physiol 1960;31:1345.
[6] Jones DRH, Chadwick GA. Experimental measurement of solid–liquid interfacial energies of transparent materials. Phila Mag 1970;22:291.
[7] Nash GE, Glicksman ME. A general method for determining solid–liquid interfacial free energies. Phila Mag 1971;24:577.
[8] Jones DRH, Chadwick GA. Experimental measurement of solid–liquid interfacial energies: the ice–water–sodium chloride system. J Cryst Growth 1971;11:260.
[9] Schaefer RJ, Glicksman ME, Ayers JD. High-confidence measurement of solid–liquid surface energy in a pure material. Phila Mag 1975;32:725.
[10] Hardy SC. A grain boundary groove measurement of the surface tension between ice and water. Phila Mag 1977;35:471.
[11] Singh NB, Glicksman ME. Determination of the mean solid–liquid interface energy of pivalic acid. J Cryst Growth 1989;98:573.
[12] Gündüz M, Hunt JD. The measurement of solid–liquid surface energies in the Al–Cu, Al–Si, Pb–Sn systems. Acta Metall 1985;33:1651.
[13] Gündüz M, Hunt JD. Solid–liquid surface energies in the Al–Mg systems. Acta Metall 1989;37:1839.
[14] Maraşlı N, Hunt JD. Solid–liquid surface energies in the Al–$CuAl_2$, Al–$NiAl_3$ and Al–Ti systems. Acta Mater 1996;44:1085.
[15] Keşlioğlu K, Maraşlı N. Solid–liquid interfacial energy of the eutectoid β phase in the Al–Zn eutectic system. Mater Sci Eng A Struct Mater Prop Microstruct Process 2004;369:294.

[16] Keşlioğlu K, Maraşlı N. Experimental determination of solid–liquid interfacial energy for Zn solid solution in equilibrium with the Zn–Al eutectic liquid. Metall Mater Trans A Phys Metall Mater Sci 2004;35A:3665.
[17] Erol M, Maraşlı N, Keşlioğlu K, Gündüz M. Solid–liquid interfacial energy of bismuth in the Bi–Cd eutectic system. Scr Mater 2004;51:131.
[18] Keşlioğlu K, Erol M, Maraşlı N, Gündüz M. Experimental determination of solid–liquid interfacial energy for solid Cd in Bi–Cd liquid solutions. J Alloys Compd 2004;385:207.
[19] Bayender B, Maraşlı N, Çadırlı E, Şişman H, Gündüz M. Solid–liquid surface energy of pivalic acid. J Cryst Growth 1998;194:119.
[20] Maraşlı N, Keşlioğlu K, Arslan B. Solid–liquid interface energies in the succinonitrile and succinonitrile–carbon tetrabromide eutectic system. J Cryst Growth 2003;247:613.
[21] Ocak Y, Akbulut S, Böyük U, Erol M, Keşlioğlu K, Maraşlı N. Measurement of solid–liquid interfacial energy for solid D camphor solution in equilibrium with succinonitrile D camphor eutectic liquid. Scr Mater 2006;55:235.
[22] Akbulut S, Ocak Y, Böyük U, Erol M, Keşlioğlu K, Maraşlı N. Solid–liquid interfacial energy of pyrene. J Appl Physi 2007;100:123505.
[23] Touloukian YS, Powell RW, Ho CY, Klemens PG. Thermal conductivity metallic elements and alloys, vol. 1. New York: Washington; 1970, pp. 39–40.
[24] Touloukian YS, Powell RW, Ho CY, Klemens PG. Thermal conductivity metallic elements and alloys, vol. 1. New York: Washington; 1970, p. 149.
[25] Porter DA, Easterling KE. Phase transformations in metals and alloys. UK: Van Nostrand Reinhold Co. Ltd; 1991. p. 204.
[26] McCartney D.G., 1981 D. Phil. Thesis, University of Oxford UK 85.
[27] Erol M, Keşlioğlu K, Şahingöz R, Maraşlı N. Experimental determination of thermal conductivity of solid and liquid phases in Bi–Sn and Zn–Mg binary eutectic alloys. Metals Miner Int 2005;11:421.
[28] Christian JW. The theory of transformations in metals and alloys part I. 2nd edn. Oxford: Pergamon; 1975. p. 169.
[29] Hansen M, Anderko K. Constitutions of binary alloys. New York: McGraw-Hill Book Company; 1958. p. 303.
[30] Tassa M, Hunt JD. The measurement of Al–Cu dendrite tip and eutectic interface temperatures and their use for predicting the extent of the eutectic range. J Cryst Growth 1976;34:38.